Eur. Phys. J. D **8**, 41–47 (2000)

THE EUROPEAN PHYSICAL JOURNAL D

EDP Sciences

Lithium vapour excitation at 2S→3D two-photon resonance

I. Labazan and S. Milošević[a]

Institute of Physics, P.O. Box 304, 10000 Zagreb, Croatia

Received 29 December 1998

Abstract. We report study of processes which occur in lithium vapour under two-photon excitation of the Li(3D) state at 639.1 nm. A time-resolved technique has been used to measure the fluorescence from the Li(3D), Li(2P) and Li(3P) states. We have determined radiation rates for lithium atom densities in the range 10^{13}–10^{14} cm^{-3} and laser powers (10^5–10^6 Wcm^{-2}). The ground-state lithium atom density was determined by knowing temperature and vapour pressure in a modified heat-pipe oven. The contribution to radiation rates from different processes and prospect for cross-section determination of homonuclear reverse energy-pooling are discussed.

PACS. 34.90.+q Other topics in atomic and molecular collision processes and interactions – 34.50.Rk Laser-modified scattering and reactions

1 Introduction

Two-photon excitation of Li(3D) state is starting point for variety of processes in lithium vapour. Under conditions of high atom densities (10^{15} cm^{-3}) and laser powers (10^6 W/cm^2) this excitation plays important role in laser plasma production [1–3]. Above atom densities of 4×10^{16} cm^{-3} stimulated hyper Raman scattering could be observed [4]. In the beam experiment associative ionization of cold 3D lithium atoms has been observed with high rate constant [5].

Our interest in this work is to identify the most probable processes at lower atom densities (10^{13} cm^{-3}) and laser powers (10^5 W/cm^2), especially those of collisional energy transfer (ET) and energy pooling (EP). Expected exothermic ET processes can be represented by following relations:

$$\mathrm{Li(3D)} + \mathrm{Li(2S)} \rightarrow \mathrm{Li(3P)} + \mathrm{Li(2S)} + \Delta E \qquad (1)$$

$$\mathrm{Li(3D)} + \mathrm{RG} \rightarrow \mathrm{Li(3P)} + \mathrm{RG} \qquad (2)$$

where RG represents rare gas atom and $\Delta E = 357.7$ cm^{-1}. The rate coefficients of these processes have been measured under different experimental conditions [6–8].

Other type of energy transfer collision is reverse energy pooling (REP) collision in which an atom prepared in highly excited state collides with an atom in the ground state, and the result is two excited atoms:

$$\mathrm{Li(3D)} + \mathrm{Li(2S)} \underset{\mathrm{EP}}{\overset{\mathrm{REP}}{\rightleftarrows}} \mathrm{Li(2P)} + \mathrm{Li(2P)} + \Delta E \qquad (3)$$

exothermic with $\Delta E = 1475$ cm^{-1}. This process is considered important for initiating the formation of a large pool of Li(2P) atoms upon 610.3 nm quasiresonant CW excitation of lithium vapour [2]. EP in lithium vapour has recently been observed, but the cross-section was not determined due to the large uncertainty regarding the Li(2P) atom density [9].

EP processes, in which two excited atoms collide and produce one highly excited atom and one ground-state atom have been studied extensively in alkali-metal vapours for both homonuclear and heteronuclear collisions [10–12]. The importance of REP collisions has recently been notified in the example of heteronuclear Na–K case [13].

In the present experiment we use a pulsed dye laser pumped with excimer laser to excite the Li(3D) level by two-photon absorption at 639.1 nm. Lithium vapour is prepared in a modified heat-pipe oven. Density of lithium vapour was in the range 10^{13}–10^{14} cm^{-3}. We detect temporal evolution of the fluorescence from the Li(2P), Li(3D), and nearby states. Our interest in this work is primary to determine conditions (namely atom densities, laser energy etc.) for the processes of equation (3) to be discernible from other processes, equations (1, 2), because of its eventual importance in understanding ionization and laser guiding discharge experiments in lithium vapour.

The article is organized in the following way. In Section 2 the experimental set up and measurement technique are described. In Section 3 we present rate-equation model used to describe expected processes. In Section 4 we show our experimental results along with a discussion of various processes involved. Finally our conclusions are presented in Section 5.

[a] e-mail: slobodan@ifs.hr

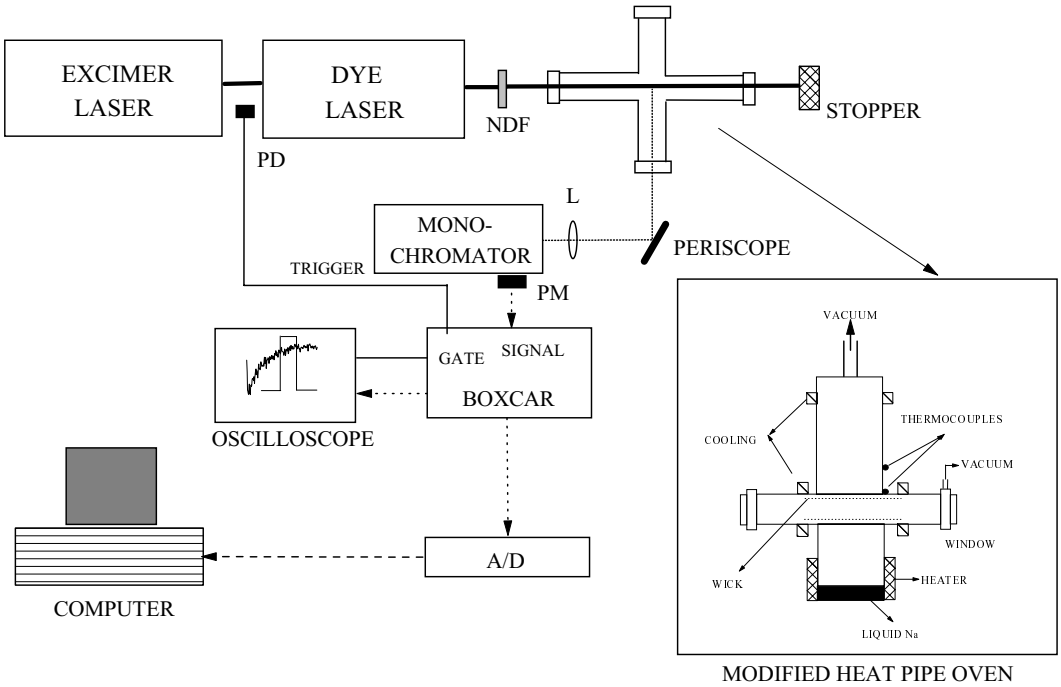

Fig. 1. Experimental arrangement for two-photon excitation in lithium. PD: fast photodiode, PM: photomultiplier, NDF: neutral density filters, L: lens and A/D: analog-digital converter.

2 Experiment

Figure 1 shows a schematic overview of the experimental setup. It consists of a heat-pipe oven, pulsed laser system and detection system. The lithium vapour is generated by use of a modified heat-pipe oven [14], which consists of two distinct systems, vertical pipe filled with sodium and horizontal filled with lithium of natural isotope abundance. Vertical heat pipe surrounds the horizontal pipe of smaller radius. In this way homogeneous heating of the horizontal heat-pipe with well defined temperature and vapour column is obtained. Sodium vapour in the vertical heat pipe is in equilibrium with buffer gas (argon in our case), so we measure the pressure of sodium vapour by measuring the pressure of the buffer gas (from 3–20 torr). From sodium vapour pressure curves [15] the temperature is obtained in the range 760–880 K. Knowing the temperature, the density of lithium atoms is obtained from vapour pressure curves and ideal gas law. The use of the vertical heat pipe is crucial to control lithium vapour pressures in the range from 2×10^{-3} to 6×10^{-2} torr (atom densities 3×10^{13}–7×10^{14} cm^{-3}) which could not be possible in a standard heat-pipe oven.

Laser system consists of a dye laser (LPD 3002E Lambda Physik) working with Rhodamine 101 dye and pumped by Xe–Cl excimer laser (LPX 105E Lambda Physik) at 308 nm. The laser pulse duration was about 20 ns (FWHM), laser repetition rate was usually 5 Hz and the pulse energy measured in the front of the heat pipe was typically in the range 1–4 mJ at 639.1 nm. The bandwidth of the dye laser without etalon is about 6 GHz and with etalon about 1 GHz. The central uniform part of laser beam was isolated by an aperture and directed in the lithium vapour through the quartz window. Diameter of the laser beam through the heat-pipe oven was about 2.5 mm. Fluorescence signal was observed perpendicular to the laser beam using a monochromator (LOMO MDR-23) with 1200 grooves/mm grating. The dispersed light was detected by a photomultiplier (Hamamatsu R2949) and the photocurrent was fed into a box-car averager (Stanford SR245). The analog signal from the box-car was then converted to digital one using an A/D converter (ADD 488/8S IoTech), and stored in a PC for further processing. Simultaneously we look at our signals from a box-car at a 8-bit 150 MHz oscilloscope (HAMEG 1507). The signal for triggering of a box-car averager was obtained from a fast photodiode (Hamamatsu S4753) monitoring a small part of 308 nm laser beam.

In this experiment we performed three types of measurements. To measure laser induced fluorescence we scan the monochromator in the wavelength interval 580–700 nm upon two-photon excitation, setting specific gate and time delay value of the box-car averager. To obtain selective wavelength excitation spectra we set the monochromator at 610.35 and 670.8 nm and tuned the laser around two-photon (639.1 nm) excitation at given settings of the box-car averager. As third, time resolved intensity of fluorescence at 610.35 nm (Li(3D)–Li(2P)), 670.8 nm (Li(2P)–Li(2S)) and 323.3 nm (Li(3P)–Li(2S)), for different densities of lithium vapour is measured by using digital storage oscilloscope or scanning the time delay of a box-car gate at a given setting of the monochromator. We use neutral density filters to lower the laser beam power. Spectral response of our detection system was measured by using a standard calibrated tungsten lamp (W2KGV22i).

Table 1. Processes relevant for the Li(3D) excitation; TPA: two-photon absorption, PI: photoionization, AI: associative ionization, CI: collisional ionization, ET: energy transfer, REP: reverse energy pooling, SD: spontaneous decay. [(a)] Estimated according to equation (3) from reference [13].

process	cross-section	conditions	reference
TPA, Li(2S)+ $h\nu$ →Li(3D)	6.25×10^{-31} cm^{4}s	990 K	[18]
PI, Li(3D)+ $h\nu$ →Li$^+$	20×10^{-18} cm^2	theor.	[19]
AI, Li(3D)+Li(3D)→ $Li_2^+ + e$	7×10^{-14} cm^2	85 K	[5]
CI, Li(3D)+Li(3D)→ Li$^+$ + Li + e^-	14×10^{-14} cm^2	100 K	[5]
ET1, Li(3D)+Li(2S)←Li(3P)+Li(2S)	7.8×10^{-15} cm^2	596 K	[8]
ET2, Li(3D)+He←Li(3P)+He	4.1×10^{-16} cm^2	298 K	[7]
ET2, Li(3D)+He←Li(3P)+He	8.6×10^{-16} cm^2	596 K	[8]
ET2, Li(3D)+He→Li(3P)+He	52×10^{-16} cm^2	313 K	[6]
ET3, Li(3D)+Ar←Li(3P)+Ar	$< 10^{-19}$ cm^2	298 K	[7]
ET3, Li(3D)+Ar→Li(3P)+Ar	4.8×10^{-18} cm^2	313 K	[6]
REP, Li(3D)+Li(2S)→Li(2P)+Li(2P)	6×10^{-16} cm^2 [(a)]	800 K	[13]

3 Lithium 3D state excitation

Figure 2 shows partial energy term diagram of lithium atom and dimer together with transitions studied in this work. Transition wavelengths and natural radiation rates are taken from reference [16]. On the left are shown $X\ ^1\Sigma_g^+$ and $A\ ^1\Sigma_u^+$ potential curves of Li_2 molecule [17].

Several processes can affect Li(3D) population and its depopulation rate. All processes relevant for Li(3D) excitation are listed in Table 1. We take into account only processes for which $\Delta E \sim 2kT$, where kT is mean kinetic energy (about 550 cm^{-1} for present experimental conditions). There are several assumptions which we use for mathematical description of excitation process. If the laser pulse is sufficiently short [20,21], the density of atoms in the Li(3D) state at the time t is given by

$$[\mathrm{Li}]_{3\mathrm{D}}(t) = [\mathrm{Li}]_{3\mathrm{D}}(0)\ \mathrm{e}^{-\Gamma^*_{3\mathrm{D}}t}. \tag{4}$$

We assume that the most important source of population of the Li(3D) state is the laser excitation. Γ^*_{3d} is decay rate for the Li(3D) state. It consists generally of several parts:

$$\Gamma^*_{3\mathrm{D}} = \Gamma^{\mathrm{rad}}_{3\mathrm{D}} + k_{\mathrm{REP}}[\mathrm{Li}]_{2\mathrm{S}} + k_{\mathrm{ET}}[\mathrm{Li}]_{2\mathrm{S}} + k_{\mathrm{RG}}[\mathrm{RG}] + \sigma_{\mathrm{PI}} I/h\nu \tag{5}$$

where I is the laser power in W/cm^2, $h\nu$ photon energy and RG stands for processes ET2 and ET3 (see Tab. 1).

The first term on the right-hand side of equation (5) is radiative radiation rate of the Li(3D) state (which is not generally equal to Einstein coefficient A due to the radiation trapping), the next three terms describe depopulation of the Li(3D) state by collisional processes, and the last term depopulation due to photoionization.

Moreover, assuming that the Li(2P) is populated mostly by radiation and/or collisions with atoms which are in Li(3D) state, we can write:

$$\dot{[\mathrm{Li}]}_{2\mathrm{P}} = (\Gamma^{\mathrm{rad}}_{3\mathrm{D}} + k_{\mathrm{REP}}[\mathrm{Li}]_{2\mathrm{S}})[\mathrm{Li}]_{3\mathrm{D}}\ (\mathrm{t}) - \Gamma_{2\mathrm{P}-2\mathrm{S}}[\mathrm{Li}]_{2\mathrm{P}}(t), \tag{6}$$

$[\mathrm{Li}]_{nl}$ is the density of atoms in the state nl, and $\Gamma_{nlJ-n'l'_{J'}}$ is the effective radiation rate from the level nl_J to the level $n'l'_{J'}$. First term on the right side describes population of Li(2P) state from Li(3D) state, the second term describe depopulation of Li(2P) state due to radiative decay.

Solution of equation (6) can be represented in the form:

$$[\mathrm{Li}]_{2\mathrm{P}}\ (t) = (-\mathrm{e}^{-t\Gamma_{2\mathrm{P}-2\mathrm{S}}} + \mathrm{e}^{-t\Gamma^*_{3\mathrm{D}}})[\mathrm{Li}]_{3\mathrm{D}}\ (0) \times \frac{\Gamma^{\mathrm{rad}}_{3\mathrm{D}} + k_{\mathrm{REP}}[\mathrm{Li}]_{2\mathrm{S}}}{\Gamma_{2\mathrm{P}-2\mathrm{S}} - \Gamma^{\mathrm{rad}}_{3\mathrm{D}} - k_{\mathrm{REP}}[\mathrm{Li}]_{2\mathrm{S}}}\,. \tag{7}$$

4 Results and discussion

In this section experimental results obtained under two-photon excitation of Li(3D) state are presented. The cross-section for two-photon absorption under similar experimental conditions was determined to be 6.25×10^{-31} cm^{4}s [18]. This results with efficient Li(3D) excitation. Figure 3 shows measured fluorescence spectrum in the range 600–700 nm which was taken at density of lithium vapour of 6.6×10^{14} cm^{-3}. We observe strong emission at 610.35 nm (3D–2P) (attenuated by factor 10^3 with ND filter), molecular emission (from 610–700 nm) and emission at 670.8 (2P–2S). Intensity ratio of atomic spectral lines is about 2300:1. Spectral line at 670.8 nm could be combined result of REP process and radiative transition from Li(3D) state. We identified observed molecular lines, by using theoretical simulation of molecular spectrum for a given excitation wavelength of the dye laser, as a fluorescence from the $Li_2(A^1\Sigma_u^+)$ state which is optically

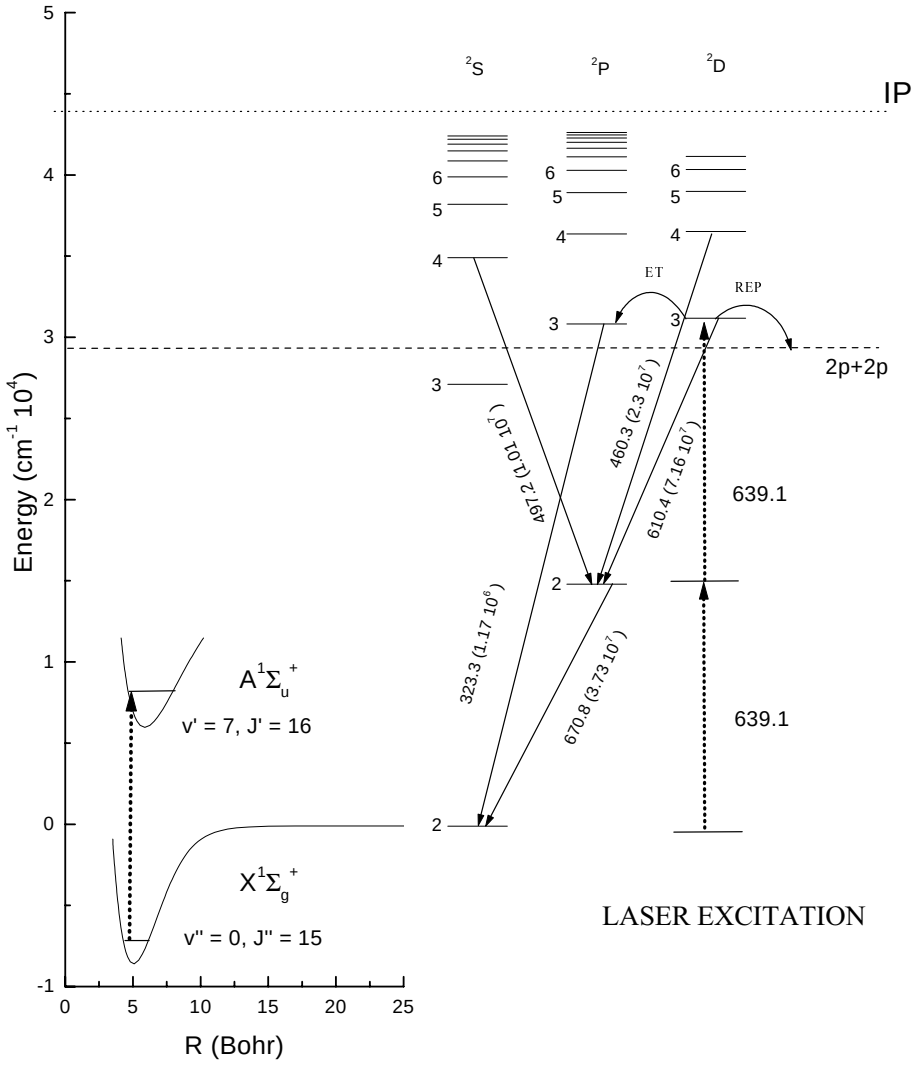

Fig. 2. Li and Li_2 energy levels and transitions relevant to the present experiment. Doted vertical arrows represent laser excitation; solid arrows represent observed radiative transitions. Wavelengths are given in nm and natural radiative rates in s^{-1} [16]. IP represents ionization potential of lithium; term diagram also shows Li(2P) + Li(2P) energy. ET and REP represent energy transfer and reverse energy pooling processes, respectively. On the left one can see X and A potential curves of Li_2 molecule taken from reference [17] and transition which is excited by 639.1 nm.

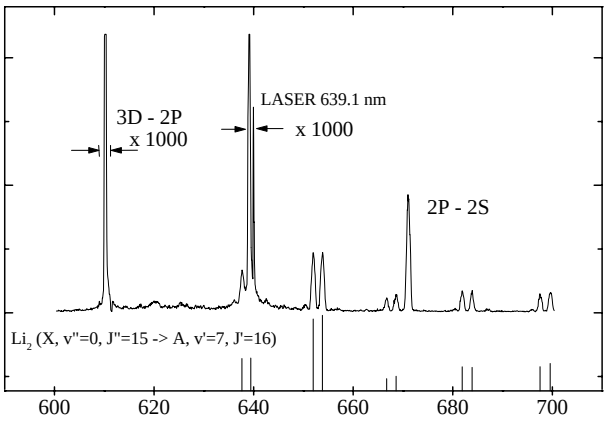

Fig. 3. Fluorescence spectrum of lithium vapour under two-photon laser excitation at 639.1 nm. Density of lithium atoms was 6.6×10^{14} cm^{-3} and vapour temperature 880 K. Laser pulse energy was 2.2 mJ. On the bottom is theoretical simulation of $^7Li_2$ molecular spectrum.

excited by following process:

$$\mathrm{Li}_2\left(X^1\Sigma_g^+, v''=0, J''=15\right)+h\nu \rightarrow \mathrm{Li}_2\left(A^1\Sigma_u^+, v'=7, J'=16\right). \quad (8)$$

Identification is performed by use of molecular constants of the X and A state given in reference [17]. Coincidence of two-photon excitation with this molecular absorption is shown in Figure 4, where we present selective excitation spectra taken with broadband laser (about 6 GHz). By tuning laser in the range 638.95–639.25 nm we record signals at 610.35 nm (Fig. 4a), at 670.8 nm (Fig. 4b) and signal at 653.6 nm ($A-X$ transition) (Fig. 4c). Emission from Li(3D) state is observed (Fig. 4a) only when the laser wavelength is exactly tuned at two-photon resonance 639.1 nm. The width of the resonance corresponds to the bandwidth of the laser. We were able to reduce the bandwidth of our laser to about 1 GHz by introducing an etalon into the dye laser resonator. At the same laser energy this results with reducing width of this resonance for about 30%. Further decrease of the width is observed by decreasing laser energy. For example

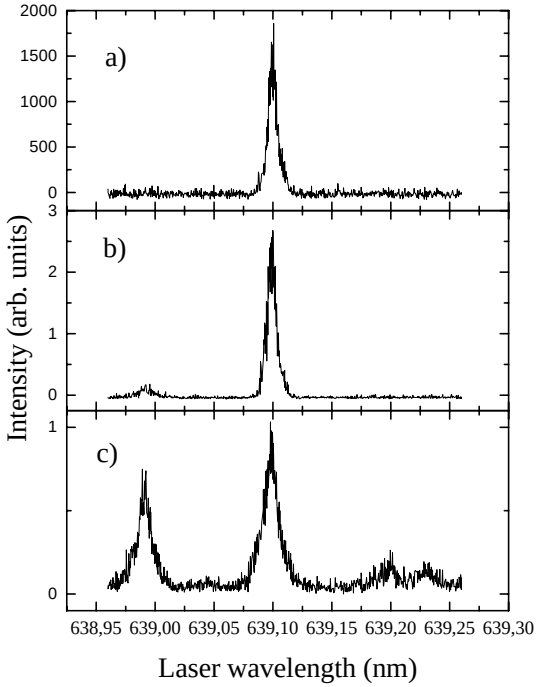

Fig. 4. Excitation spectra at 610.35 nm (a: 3D–2P), 670.8 nm (b: 2P–2S) and 653.6 nm (c: A–X band). Density of lithium atoms is 4.5×10^{14} cm^{-3}, density of Li_2 5.2×10^{12} cm^{-3}, temperature 860 K and laser pulse energy 2.2 mJ.

from 0.009 nm at about 2 mJ to 0.005 nm at 5 μJ. This clearly indicates power broadening on the two-photon absorption. The emission from Li(2P) state occurs for laser excitation wavelengths at 638.98 nm and 639.1 nm (Fig. 4b). Resonance at 638.98 nm is the result of resonant excitation of molecule-atom collisions [22]:

$$\mathrm{Li}_2\left(A^*\Sigma_u^+, v', J'\right) + \mathrm{Li(2S)} \rightarrow \mathrm{Li}_2\left(X^1\Sigma_g^+, v'', J''\right) + \mathrm{Li(2P)} + \Delta E. \quad (9)$$

In Figure 4c we see four such resonances, at 638.98 nm, 639.1 nm, 639.2 nm and 639.23 nm, which corresponds to the $X \rightarrow A$ band excitation. If we examine Figures 4a and 4c we see strong coincidence between two-photon excitation of the Li(3D) and one-photon excitation of lithium molecule from the $\mathrm{Li}_2(X^1\Sigma_g^+)$ to $\mathrm{Li}_2(A^1\Sigma_u^+)$ molecular state. Even with improved laser spectral resolution (using etalon), the coincidence of simultaneous $A-X$ band and two-photon 3D state excitation could not be avoided.

In the following we have studied the time evolution of the fluorescence at 3D–2P, 2P–2S, and 3P–2S transitions. Figure 5 shows measurements at 3D–2P and 2P–2S transition for two densities of lithium vapour, 9.6×10^{13} cm^{-3} and 3.3×10^{13} cm^{-3}. These decay curves were measured by digital storage oscilloscope which averaged 64 laser pulses. We see that the 3D–2P fluorescence signal is attenuated during the period of 500 ns. Total decay of the 2P–2S fluorescence occurs in the period of 25 μs. We believe that fast portion (up to 100 ns) of the 2P–2S signal is due to radiative decay from higher excited states. We fit equation (4) on Li(3D–2P) signals in time period 50–500 ns in order to avoid influence of directly scattered laser light and fast multiphoton processes. Equation (5) was fitted on Li(2P–2S) fluorescence signals in the time interval 50 ns–25 μs. From fits at different densities we get Stern-Volmer graph for Γ^*_{3D} and Γ_{2P} for two different laser pulse energies shown in Figure 6. These laser energies are chosen approximately in the transition region were time-integrated fluorescence intensity at 610.3 nm shows saturation effects. At larger laser energy of 2.2 mJ Γ^*_{3D} decrease with atom density and it is of the order of 10^7 s^{-1}, similar to natural radiation rate, 7.1×10^7 s^{-1}, (Fig. 6a); the slope of the linear fit is negative (-9.49×10^{-15} cm^3 s^{-1}) contrary to equation (5), indicating that $\Gamma^{\mathrm{rad}}_{3D}$ depends on the density of the Li(2S) state. This could be due to the radiation trapping on 3D–2P transition. For the same laser energy, Γ_{2P} slowly decreases with atom density and is smaller than natural radiation rate (3.73×10^7 s^{-1}) for two orders of magnitude (Fig. 6b). Such smaller radiation rate (longer lifetime) is the indication of the process of radiation trapping on the 2P–2S transition [23].

At smaller laser pulse energy of 1 mJ, Γ^*_{3D} dependence on atom density change the sign of the slope and is in accordance with equation (5) (Fig. 6c). The slope in this case of laser pulse energy is $(5.7\pm0.2)\times10^{-8}$ cm^3 s^{-1}. At this smaller laser pulse energy Γ_{2P} dependence on atom density shows maximum at 1.6×10^{14} cm^{-3}. We believe that obtained Γ^*_{3D} and Γ_{2P} dependencies on atom density and laser pulse energy are consequences of a nonlinear trapping effects [24].

To study process given with equation (2), we measured time evolution of fluorescence signals of the Li(3P–2S) at 323.3 nm *versus* density of the rare gas atoms (helium and argon). Measured radiation rates Γ^*_{3D} and Γ_{3P} are shown in Figure 7 for different laser pulse energies. In Figures 7a and 7c we see Γ_{3P} and Γ^*_{3D} dependence on He atoms density, and in Figures 7b and 7d dependence on Ar atom densities. It can be seen that Γ^*_{3D} and Γ_{3P} have almost constant value for different density of Ar atoms. This is not the case for helium, so we can conclude that to avoid large energy transfer from the Li(3D) towards the Li(3P), equation (2), argon has to be used as a buffer gas in the heat-pipe oven. This conclusion is in agreement with other works, [6–8]. The Li(3P) atom can be a source of population of the Li(2P) state through REP process with energy defect $\Delta E = 1117.38$ cm^{-1}.

We note that emission from higher levels of lithium atom (4D and 4S) at 460.3 nm and 497.2 nm could be also observed at largest atom densities and laser powers used in the present experiment. The dependence of intensities and decay rates of these emission on laser power suggests that photoionization of Li(3D) by third 639.1 nm photon followed by a radiative recombination is responsible for population of these high lying levels. Significance of the photoionization effect could be efficiently reduced by reducing laser power.

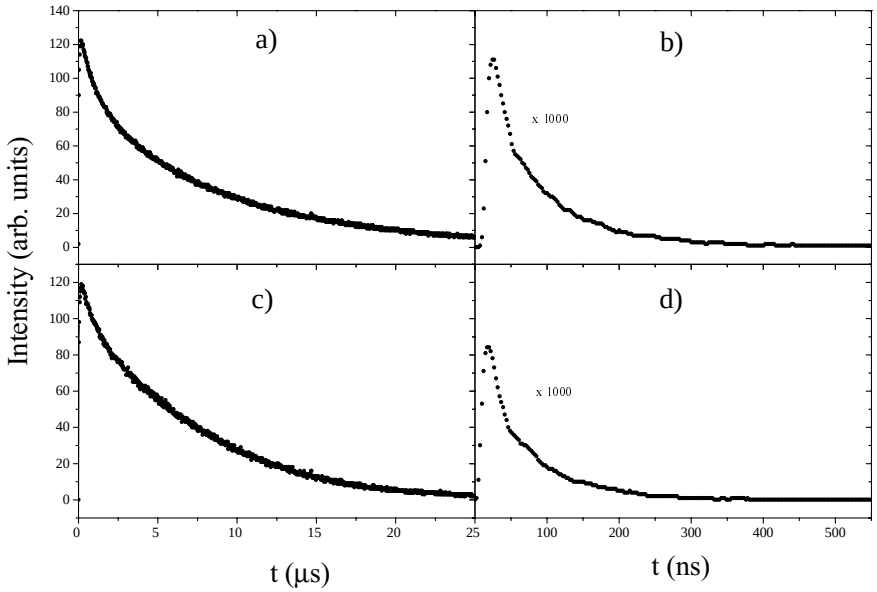

Fig. 5. Averaged time evolution of signals at 670.8 nm (2P–2S), (a, c), and 610.35 nm (3D–2P), (b, d) upon two-photon excitation of the Li(3D) state. Upper spectra (a, b), are taken at lithium atom density 9.6×10^{13} cm^{-3} ($T = 803$ K) and lower (c, d) at 3.3×10^{13} cm^{-3} ($T = 768$ K). Laser pulse energy was 2.2 mJ.

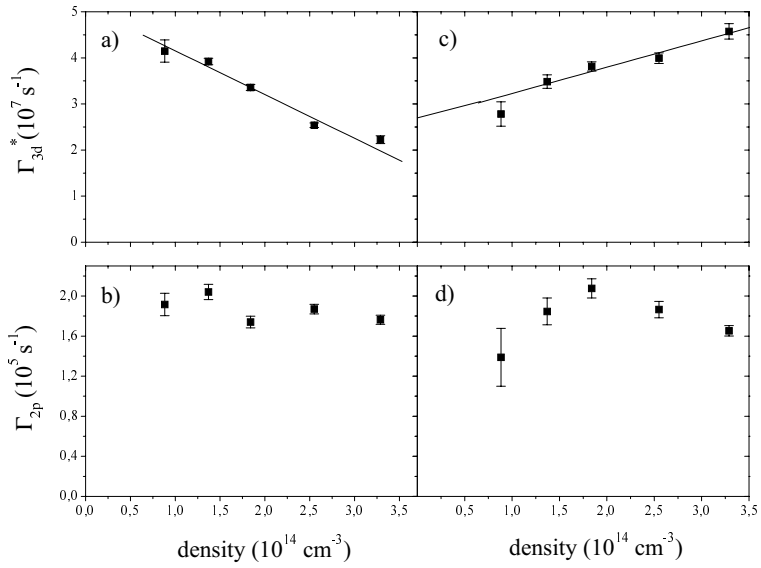

Fig. 6. Radiation rates for two-photon laser excitation *vs.* density of lithium vapour. Laser pulse energy was 2.2 mJ (left) and 1 mJ (right).

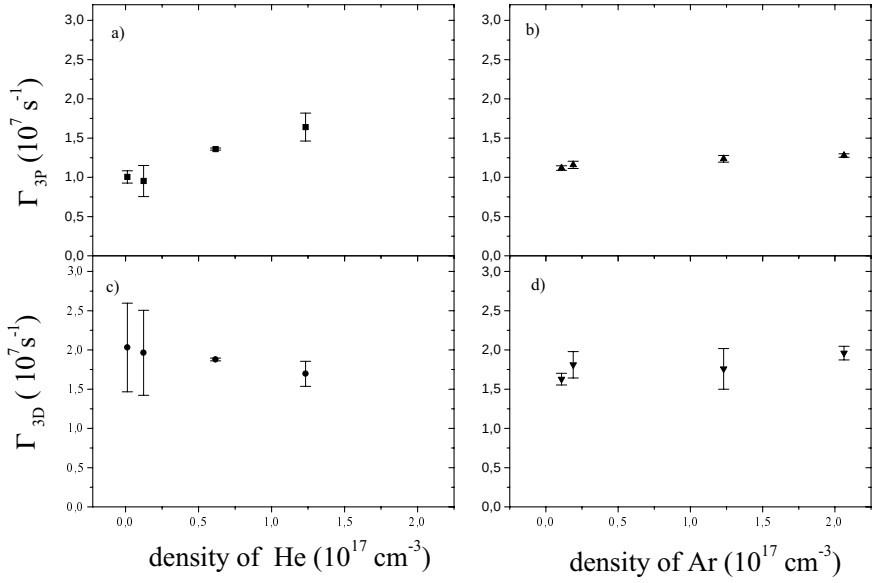

Fig. 7. Radiation rates Γ_{3P} and Γ^*_{3D} averaged over different laser energies *vs.* density of helium, (a, c); density of argon, (b, d). Density of lithium atoms was 5.5×10^{13} cm^{-3} for (a and b); 3.5×10^{13} cm^{-3} for (c and d).

5 Conclusions

We have measured radiation rates from lithium atomic states which are populated under two-photon excitation of Li(3D) state. We used a modified heat-pipe oven to precisely control a low lithium vapour pressures needed to obtain 10^{13}–10^{14} cm^{-3} atom densities. We found a strong coincidence (within 1 GHz) of atomic and molecular excitation at 639.1 nm which indicates that at larger atom densities ($> 10^{15}$ cm^{-3}) used in a laser induced plasma or discharge experiments [25], molecular ionization channels could play an important role. The decay rates of Li(3D) and Li(2P) states, which are of the order of 10^7 s^{-1} and 10^5 s^{-1} respectively, shows complicated dependence on total atom density and laser powers. This is due to an interplay of saturation, (nonlinear) radiation trapping and photoionization effects. This precludes determination of the cross-section for reverse energy pooling collision. A nonlinear radiation trapping effect can be minimized for $E_{\rm laser} < 1$ mJ and atom densities smaller than 1.5×10^{14} cm^{-3}. However at atomic density of 10^{14} cm^{-3} radiation population of the Li(2P) state dominates over the collisional energy transfer (REP). The reverse energy pooling as a source for large pool of Li(2P) atoms could be important only at larger atom densities, where radiation trapping will reduce radiation rates to 10^4 or 10^3 s^{-1}.

This work was financially supported by the Ministry of Science and Technology of the Republic of Croatia. We wish to thank Dr. Goran Pichler for valuable discussions and continuous support of this work.

References

1. W.C. Stwalley, J.T. Bahns, in *Laser and Particle Beams* (Cambridge University Press, 1993), Vol. 11, p. 185.
2. D. Veza, C.J. Sansonetti, Z. Phys. D **22**, 463 (1992).
3. M.E. Koch, C.B. Collins, Phys. Rev. A **19**, 1098 (1979).
4. D. Krökel, K. Ludewigt, H. Welling, IEEE J. Q. Electron. **22**, 489 (1986).
5. M.W. McGeoch, R.E. Schlier, G.K. Chawla, Phys. Rev. Lett. **61**, 2088 (1988).
6. W.J. Wang, M.D. Havey, Phys. Rev. A **29**, 3184 (1984).
7. N. Yonekura, T. Nakajima, Q. Hui, M. Takami, Chem. Phys. Lett. **280**, 525 (1997).
8. C. Chaleard, B. Dubreuil, A. Catherinot, Phys. Rev. A **26**, 1431 (1982).
9. C. He, R.A. Bernheim, Chem. Phys. Lett. **190**, 494 (1992).
10. Z.J. Jabbour, R.K. Namiotka, J. Huennekens, M. Allegrini, S. Milošević, F. de Tomasi, Phys. Rev. A **54**, 1372 (1996).
11. C. Gabbanini, S. Gozzini, G. Squadrito, M. Allegrini, L. Moi, Phys. Rev. A **39**, 6148 (1989).
12. R.K. Namiotka, J. Huennekens, M. Allegrini, Phys. Rev. A **56**, 514 (1997).
13. G. De Filippo, S. Guldberg-Kjær, S. Milošević, J.O.P. Pedersen, M. Allegrini, Phys. Rev. A **57**, 255 (1998).
14. H. Scheingraber, C.R. Vidal, Rev. Sci. Instrum. **52**, 1010 (1981).
15. A.N. Nesmeyanov, *Vapour Pressure of Chemical Elements* (Elsevier, New York, 1963).
16. W.L. Wiese, M.W. Smith, B.M. Glennon, *Atomic Transition Probabilities* (National Bureau of Standards, Washington, DC, 1966), Vol. I, p. 17.
17. P. Kusch, M.M. Hessel, J. Chem. Phys. **67**, 586 (1977).
18. G.C. Tisone, P.J. Hargis Jr, AIP Conf. Proc. **160**, 404 (1987).
19. M. Aymar, E. Luc-Koenig, F. Combet Farnoux, J. Phys. B: At. Mol. Phys. **9**, 1279 (1976).
20. A. Kopystyńska, P. Kowalczyk, Opt. Commun. **25**, 351 (1978).
21. J. Huennekens, A. Gallagher, Phys. Rev. A **27**, 1851 (1983).
22. J. Derouard, N. Sadeghi, Chem. Phys. Lett. **111**, 353 (1984).
23. A.F. Molisch, B.P. Oehry, W. Schupita, G. Magerl, J. Quant. Spectrosc. Radiat. Transfer **49**, 361 (1993).
24. N.N. Bezuglov, A.N. Klucharev, A.F. Molisch, M. Allegrini, F. Fuso, T. Stacewicz, Phys. Rev. E **55**, 3333 (1997).
25. H. Skenderović, T. Ban, G. Pichler, Opt. Commun. **161**, 217 (1999).